ISSN 1063-7761, Journal of Experimental and Theoretical Physics, 2020, Vol. 130, No. 2, pp. 235–246. © Pleiades Publishing, Inc., 2020.
Russian Text © The Author(s), 2020, published in Zhurnal Eksperimental'noi i Teoreticheskoi Fiziki, 2020, Vol. 157, No. 2, pp. 281–294.

ORDER, DISORDER, AND PHASE TRANSITION IN CONDENSED SYSTEM

Gapless Chiral Superconducting ($d + id$)-Wave Phase in Strongly Correlated Layered Material with a Triangular Lattice

V. V. Val'kov[a,*], T. A. Val'kova[b], and V. A. Mitskan[a,c]

[a] *Kirensky Institute of Physics, Federal Research Center "Krasnoyarsk Scientific Center," Siberian Branch, Russian Academy of Sciences, Krasnoyarsk, 660036 Russia*

[b] *Siberian Federal University, Krasnoyarsk, 660041 Russia*

[c] *Reshetnev Siberian State University of Science and Technology, Krasnoyarsk, 660037 Russia*

**e-mail: vvv@iph.krasn.ru*

Received July 4, 2019; revised August 26, 2019; accepted August 27, 2019

Abstract—It is shown that interlayer electron tunneling in the quasi-two-dimensional ensemble of Hubbard fermions leads to the realization of the gapless superconducting phase with the chiral ($d + id$)-wave order parameter symmetry, not for a single value of sodium ion concentration, but in a wide range of concentrations. Precisely this situation corresponds to experimental data on the layered sodium cobaltite intercalated by water ($Na_xCoO_2 \cdot yH_2O$). Intra-atomic electron repulsion that determines the strong electron correlation regime leads to the representation of Hubbard fermions, the interaction of which ensures Cooper instability. Intersite intralayer interactions between fermions considerably affect the positions of nodal points of the chiral order parameter and change the critical concentration at which a topological transition occurs in the 2D system of Hubbard fermions.

DOI: 10.1134/S1063776120010197

1. INTRODUCTION

Layered magnets in which spins in planes are localized at the triangular lattice sites are systems with quantum effects that are manifested at the macroscopic level. This is due to strongly developed fluctuations associated with frustrated exchange bonds on the triangular lattice as well as with the quasi-2D structure. These factors determine nontrivial properties of layered materials with a triangular lattice and induce heightened interest from many research groups [1–9].

In conducting quasi-2D strongly correlated materials with a triangular lattice, the engaging of the Fermi degrees of freedom leads to new nontrivial effects. The superconducting phase [10] with the chiral symmetry of the order parameter becomes a candidate for the fundamental state of the system. This symmetry type in combination with the noncollinear spin ordering make possible the nontrivial topology and Majorana modes [12–15]. In view of strong electron correlations, additional features appear in the electromagnetic response [16] and thermomagnetic properties [17] of the superconducting phase formed due to exchange of spin excitations [18]. A spin density wave that can appear in the electron system described by the Hubbard model [19] on a triangular lattice can initiate the pseudogap behavior [20] of such an electron ensemble. The existence of the d-wave superconductivity in such systems was confirmed by calculations based on quantum dynamic cluster Monte Carlo methods [21].

The discovery of a transition to the superconducting phase with an anisotropic order parameter in water-intercalated sodium cobaltite $Na_xCoO_2 \cdot yH_2O$ at $T_c = 5$ K [10] substantially increased the number of experimental [22–25] and theoretical investigations [26–29] of properties of the normal and superconducting phases in quasi-two-dimensional materials with a triangular lattice.

In particular, considerable attention was paid to the symmetry of the superconducting order parameter (SOP) (see reviews [30–32]). Since the triangular lattice symmetry permits the realization of the chiral ($d_{x^2-y^2} + id_{xy}$)-wave SOP symmetry, the question concerning the presence (or absence) of the gap in the Fermi excitation spectrum of such a superconducting phase arose.

It is assumed that the single-orbital Hubbard model [19] is the minimal model for describing the electronic structure of the CoO_2 plane. In the strong electron correlation regime, when the energy of the intraatomic Coulomb electron repulsion (characterized by parameter U) is much higher than the absolute value of hopping integrals t_{fm}, the effective model is used. This model can be constructed, for example, using the unitary transformation method [33, 34] or

the operator form of perturbation theory in the form of expansion in smallness parameters t_{fm}/U. In this case, second-order parameters contain two- and three-center operators. If three-center terms are discarded, we have the so-called t–J model [33, 34]. If, however, three-center terms are included, there appears the t–J^* model. It is important that three-center terms are also proportional to $(t_{fm}/U)^2$ and, hence, considerably affects the conditions for the realization of the superconducting d-wave phase [35].

Analysis of the properties of the superconducting phase with a complex order parameter on a triangular lattice, which is performed based on the t–J model [26–28] combined with the results of other theoretical works [30–32], necessitated correcting of the chosen methods for describing the superconducting state.

The reason for this has become obvious in the attempt at matching the time evolution of the spin–lattice relaxation obtained from the observation of the nuclear magnetic resonance in $Na_xCoO_2 \cdot yH_2O$ with the concept of the singlet nature of Cooper pairing and the chiral $(d + id)$-wave of the SOP symmetry.

As a matter of fact, the interaction between fermions in the aforementioned publications was considered only within the first coordination sphere. In this case, the nodal points of the SOP lie only at the center and at the edges of the Brillouin zone. For this reason, the spectrum in the superconducting phase has a gap for any doping level, while the spin–lattice relaxation data required that superconductivity be gapless.

An approach to overcoming the difficulty with the indication of the mechanism of realization of the gapless Fermi excitation spectrum for chiral $(d + id)$-wave superconductors with a triangular lattice was proposed in [11]. The main hypothesis formulated in [11] was that the superconducting pairing occurs only for fermions at the next-to-nearest sites. In this case, the SOP nodal points lie within the Brillouin zone. Then the spectrum for the superconducting phase for the fermion concentration at which the Fermi contour of the normal phase intersects the SOP zeros becomes gapless and is characterized by six Dirac points.

However, the proposed mechanism of formation of the gapless $(d + id)$-wave superconductivity does not solve the above problem completely, not to mention its somewhat artificial nature. As a matter of fact, the above scenario of formation of the gapless phase is realized only for one fermion concentration, while the experimental matching between the theory and experiment requires that the gapless spectrum be realized in a wide range of doping with sodium ions.

The possibilities of formation of SOP nodal points within the Brillouin zone were extended by considering a more realistic situation in which the potentials of Cooper pairing of fermions from two coordination spheres are accounted for simultaneously [36]. With such an approach, there appears a dependence of the positions of the SOP nodal points in the Brillouin zone on the model parameters as well as generally on the doping level. This substantially extended the functional potentialities of the theory in improving the agreement with experimental data. However, the main goal (viz., theoretical description of the gapless chiral superconducting $(d + id)$-wave phase for a triangular lattice in a wide doping level interval) was not achieved.

In this study, we propose the solution of the aforementioned problem. The main idea is associated with the account for the actual quasi-two-dimensional nature of the crystallographic structure of the materials in question. In this case, condition $|t_\perp| \ll |t|$ turned out to be significant, where $t_\perp$ is the parameter of electron hopping between nearest sites in the direction perpendicular to the layers and t is the largest electron hopping integral in the plane of the layer. This inequality leads to the situation in which the superexchange coupling between magnetically active ions located in the same layer, which is proportional to the square of the hopping parameter, is substantially larger than the analogous coupling between such ions belonging to different layers. This permits the use of the model in which the Fermi excitation spectrum of the normal phase is formed on the basis of the quasi-two-dimensional crystallographic structure, while, as regards superconducting pairing potentials, this model describes a system of uncoupled layers with a triangular lattice.

The article is organized as follows. In Section 2, we consider the model of the electronic structure of an individual CoO_2 layer with account for strong electron correlations and pass to an ensemble to the Hubbard fermions. The derivation of the self-consistency equation for the superconducting order parameter using the diagram technique for the Hubbard operation is described in Section 3. In Section 4, we construct the region of realization of the chiral superconducting phase in the 2D ensemble of the Hubbard fermions and analyze possible configurations of nodal points of the superconducting order parameter. The concentration evolution of nodal points is considered in Section 5 with count for the intersite Coulomb repulsion of fermions. In Section 6, we demonstrate that the inclusion of interlayer hops in the quasi-two-dimensional ensemble of Hubbard fermions leads to realization of the gapless chiral superconducting phase in a wide concentration range as is observed in experiments. The results are summarized in Conclusions.

2. QUASI-TWO-DIMENSIONAL ENSEMBLE OF HUBBARD FERMIONS

Cobalt ions in the CoO_2 planes nominally correspond to the four-valent state (Co^{4+}) with the $3d^5$ electron configuration. Because of the presence of trigonal distortion, the lower orbital triplet formed in the octahedral crystal field splits into the upper singlet level

and the lower doubly degenerate level. Accordingly, four d-electrons of the Co^{4+} ions occupy the lower states (considering spin degrees of freedom), while the remaining electron participates (during the formation of CoO_2 layer) in filling of the band states formed as a result of collectivization of the upper states.

Under the influence of the intra-atomic Coulomb repulsion, the aforementioned simple pattern of one-fermion band states is modified. The main manifestation of such a modification is known to be described by the single-orbital Hubbard model [19]. This, however, is insufficient for reflecting the features of the superconducting phase of sodium cobaltite (see below), and we must take into account the Coulomb interaction of electrons located at different sites. For this reason, we will use the Shubin–Vonsovski model [37–39]

$$H = \sum_{f\sigma}(\varepsilon - \mu)\hat{n}_{f\sigma} + \sum_{f} U\hat{n}_{f\uparrow}\hat{n}_{f\downarrow} + \sum_{fm\sigma} t_{fm}a^{+}_{f\sigma}a_{m\sigma} + \sum_{fm} V_{fm}\hat{n}_f\hat{n}_m. \quad (1)$$

Here, $\hat{n}_{f\sigma} = a^{+}_{f\sigma}a_{f\sigma}$ is the operator of the number of electrons with spin projection σ at site f of the 3D lattice, $a^{+}_{f\sigma}$ ($a_{f\sigma}$) is the creation (annihilation) operator for electron with spin projection σ at site f; ε is the initial energy of the one-electron state; μ is the chemical potential of the electron system, and U is the Hubbard repulsion energy of electrons located on the same Vanier orbital with opposite spin projections.

The intersite interaction of electrons is described by the last term in the second line in expression (1), $\hat{n}_f = \hat{n}_{f\uparrow} + \hat{n}_{f\downarrow}$ is the operator of the total number of electrons on site f, and V_{fm} is the parameter of interaction between electrons located on sites f and m.

In the kinetic energy operator, parameter t_{fm} describes the intensity of an electron hop from site m to site f.

An increase in concentration x of sodium ions in $Na_xCoO_2 \cdot yH_2O$ leads to the passage of a part of cobalt ions to state Co^{3+} with electron configuration $3d^6$. In accordance with the hierarchy of the kinetic states of electrons at cobalt ions considered above, we find that doping is accompanied by the filling of the upper Hubbard subband. In this case, the role of the single-site basis for the Hilbert subspace is played by singly filled electron states $|\uparrow\rangle$ and $|\downarrow\rangle$, as well as "two" states $|2\rangle$.

Accordingly, in the regime of strong electron correlations ($U \gg |t_{fm}|, |t_\perp|$), in solving problem of the structure of collectivized Fermi states in sodium cobaltite, we can pass to the description in the language of singly and doubly filled single-site states in the framework of the effective Hamiltonian.

A transition to the effective Hamiltonian acting in the truncated Hilbert space can be realized rigorously using the operator form of perturbation theory [40].

Taking into account the second-order terms in $|t_{fm}|/U$ inclusively, we obtain a model representing the Hubbard fermion ensemble:

$$H_{\text{eff}} = H_0 + \hat{T} + \hat{J} + \hat{J}^* + \hat{V}. \quad (2)$$

The first term

$$H_0 = \sum_{f\sigma}(\varepsilon - \mu)X^{\sigma\sigma}_f + \sum_{f}(2\varepsilon + U - 2\mu)X^{22}_f \quad (3)$$

describes one- and two-electrons states at the sites of the 3D lattice in the atomic representation [41, 42].

Operator

$$\hat{T} = \sum_{fm\sigma} t_{fm}X^{2\bar{\sigma}}_f X^{\bar{\sigma}2}_m \quad (4)$$

takes into account the hops between the Hubbard fermion sites.

The third term of H_{eff} reflects the emergence of exchange coupling between cobalt ions in the second order of perturbation theory ($J_{fm} = 2t_{fm} \cdot t_{mf}/U$):

$$\hat{J} = \frac{1}{2}\sum_{fm\sigma} J_{fm}(X^{\bar{\sigma}\sigma}_f X^{\sigma\bar{\sigma}}_m - X^{\bar{\sigma}\bar{\sigma}}_f X^{\sigma\sigma}_m). \quad (5)$$

The operator with three-center terms,

$$\hat{J}^* = \sum_{\substack{fmg\sigma \\ (f\neq g)}} \frac{t_{fm}t_{mg}}{U}(X^{2\bar{\sigma}}_f X^{\sigma\sigma}_m X^{\bar{\sigma}2}_g - X^{2\bar{\sigma}}_f X^{\bar{\sigma}\sigma}_m X^{\sigma 2}_g), \quad (6)$$

which is obtained in the same order of perturbation theory, described correlated hops of Hubbard fermions.

The correlated part of the intersite Coulomb interaction between such fermions can be expressed in terms of operator

$$\hat{V} = \frac{1}{2}\sum_{f\delta} V(\hat{n}_f - \langle\hat{n}_f\rangle)(\hat{n}_{f+\delta} - \langle\hat{n}_{f+\delta}\rangle), \quad (7)$$

in which the operator of the number of electrons at site f is defined as

$$\hat{n}_f = X^{\uparrow\uparrow}_f + X^{\downarrow\downarrow}_f + 2X^{22}_f.$$

Hubbard operators $X^{pq}_f = |f, p\rangle\langle f, q|$ are defined conventionally using the basis of atomic states such that $|f, p\rangle$ is one of three possible states at site f.

In further analysis, we will consider the Coulomb interaction only for electrons located within one layer. The Coulomb interaction between electrons from different layers will be ignored because of screening effects since the spacing between the layers increases significantly during intercalation due to embedding of water molecules between the CoO_2 planes.

For the same reason, we assume that the interlayer electron tunneling is much weaker than tunneling of

electrons between the sites located within one CoO_2 plane. Accordingly, parameter $t_\perp$ determining the intensity of an electron transition between the nearest sites will be assumed modulo smaller than the hopping parameter in one plane. We assume for simplicity that interlayer hops occur only between the sites located in neighboring CoO_2 layers.

In this case, the exchange interaction between cobalt ions located in different CoO_2 layers is disregarded because, in view of condition $t_\perp \ll |t|$ ($|t|$ is the modulo largest hopping parameter $|t_{fm}|$ within a plane), the interlayer exchange coupling parameter is much smaller than the intralayer parameter. The interaction between the layers is important in analysis of the magnetically ordered phase at finite temperatures.

In further analysis, we will disregard correlated hops between the layers is disregarded for the reason given in the description of operator $\hat{J}$.

Considering the above arguments, we come to the conclusion that the features of the superconducting phase of sodium cobaltite are determined by peculiarities of the quasi-two-dimensional ensemble of Hubbard fermions with a triangular lattice in CoO_2 layers. The inclusion of strong single-site electron correlations is reflected in the transition to the X operators that are known to possess other algebra of permutation relations. The use of the concept of Hubbard fermions introduced above is associated with this circumstance.

3. EQUATION FOR THE ORDER PARAMETER OF THE CHIRAL SUPERCONDUCTING PHASE

The self-consistency equation for the order parameter in the superconducting phase can be derived with the help of the Matsubara Green functions (GFs) in the atomic representation [42]:

$$D_{\alpha,\beta}(f\tau, g\tau') = -\langle T_\tau \tilde{X}_f^\alpha(\tau)\tilde{X}_g^{-\beta}(\tau')\rangle = \frac{T}{N}\sum_{k,\omega_n} e^{ik(f-g)-i\omega_n(\tau-\tau')} D_{\alpha,\beta}(k, i\omega_n), \quad (8)$$

where the angle brackets in the first line indicate averaging over the grand canonical ensemble defined by statistical operator

$$\rho = \exp(-H_{\text{eff}}/T)$$

with temperature T. Operator T_τ chronologizes the products of the Hubbard operators in the Heisenberg representation in Matsubara "temporal" variables τ and τ':

$$\tilde{X}_f^\alpha(\tau) = \exp(\tau H_{\text{eff}}) X_f^\alpha \exp(-\tau H_{\text{eff}}).$$

Indices α and β (root vectors [42]) are used for denoting transitions between single-site states $|\uparrow\rangle$, $|\downarrow\rangle$, and $|2\rangle$ and, hence, depend on two numbers of these states: $\alpha = \alpha(n, m)$. In this case,

$$X_f^\alpha = X_f^{\alpha(n,m)} = X_f^{nm}.$$

Acting on the wavefunction of the system, such an operator transforms state $|m\rangle$ of site f to state $|n\rangle$ of the same site. The negative value of root vector $-\beta = -\beta(n, m)$ corresponds to the inverted transition of a cobalt ion from single-site state $|n\rangle$ into single-site state $|m\rangle$; i.e.,

$$X_f^{-\beta(n,m)} = X_f^{\beta(m,n)} = X_f^{mn}.$$

In the second line of definition (8), the Fourier transform of the Matsubara Green function is introduced in atomic representation, $D_{\alpha,\beta}(k, i\omega_l)$, in which k is the quasi-momentum and $\omega_l = (2l + 1)\pi T$, $l = 0, \pm1, \pm2, \ldots$, is the Matsubara frequency for anticommuting operators.

If functions $D_{\alpha,\beta}(k, i\omega_n)$ are treated as elements of matrix $\hat{D}(k, \omega_l)$, analysis of the diagrammatic series for $D_{\alpha,\beta}(k, i\omega_l)$ leads to matrix equation

$$\hat{D}(k, i\omega_l) = \hat{G}(k, i\omega_l)\hat{P}(k, i\omega_l), \quad (9)$$

where $\hat{P}(k, i\omega_l)$ is the force operator [42, 43]. Function $\hat{G}$ satisfies the Dyson equation in conventional form

$$\hat{G}(k, i\omega_l) = \hat{G}^{(0)}(k, i\omega_l) + \hat{G}^{(0)}(k, i\omega_l)\hat{\Sigma}(k, i\omega_l)\hat{G}(k, i\omega_l),$$

where $\hat{\Sigma}(k, i\omega_l)$ is the mass operator, and collectivized Green function

$$\hat{G}^{(0)}(k, i\omega_l) = \{[\hat{G}_0(k, i\omega_l)]^{-1} - \hat{P}(k, i\omega_l)\hat{t}_k\}^{-1}$$

describes noninteracting quasiparticles of the normal phase if the force operator is calculated in the mean-field approximation, and $\hat{G}_0(i\omega_l)$ is the matrix of single-site propagators

$$(\hat{G}_0(i\omega_l))_{\alpha\beta} = \delta_{\alpha\beta}[i\omega_l + E_n - E_m]^{-1}, \quad \alpha = \alpha(n, m),$$

E_n and E_m being the initial one-ion energies. Matrix $\hat{t}_k$ is composed of the Fourier transforms of elements $t_{fg}^{\alpha\beta}$, the values of which can be determined from comparison of operator $\hat{T}$ with the same operator written in form

$$\hat{T} = \sum_{fg}\sum_{\alpha\beta} t_{fg}^{\alpha\beta} X_f^{-\alpha} X_g^\beta.$$

We will confine our further analysis to the mean-field approximation corresponding to the Gor'kov theory for traditional superconductors [44]. For the sake of brevity, we will denote normal GF $G_{\downarrow 2,\downarrow 2}$ by G and anomalous GF $G_{\downarrow 2,2\uparrow}$ by F.

Denoting the anomalous component of the mass operator by $\Delta(k)$, we obtain from the Dyson equation

$$F(k, i\omega_l) = \frac{\Delta(k)}{(i\omega_l)^2 - E_k^2}, \quad (10)$$

where

$$E_k = \sqrt{\xi_k^2 + |\Delta(k)|^2} \quad (11)$$

is the Fermi excitation spectrum in the superconducting phase. For the t–J–V model, the normal phase spectrum measured from the chemical potential is defined as

$$\xi_k = \varepsilon + U + \frac{1+x}{2} t_k - \mu, \quad (12)$$

while for the t–J^*–V model, we have

$$\xi_k = \varepsilon + U + \frac{1+x}{2} t_k + \frac{(1-x^2)}{4} t_k^2 - \mu, \quad (13)$$

where x is the fraction of two-states in the Hubbard fermion ensemble, which is connected with the electron concentration n on a site by relation $x = n - 1$. The Fourier transform of hopping integral t_k with account for parameters t_1, t_2, and t_3 for three coordination spheres is written as

$$t_k = 2t_1\varphi_{s1}(k) + 2t_2\varphi_{s2}(k) + 2t_3\varphi_{s3}(k), \quad (14)$$

where

$$\varphi_{s1}(k) = \cos k_y + 2\cos\left(\frac{\sqrt{3}k_x}{2}\right)\cos\left(\frac{k_y}{2}\right),$$

$$\varphi_{s2}(k) = \cos(\sqrt{3}k_x) + 2\cos\left(\frac{\sqrt{3}k_x}{2}\right)\cos\left(\frac{3k_y}{2}\right), \quad (15)$$

$$\varphi_{s3}(k) = \cos(2k_y) + 2\cos(\sqrt{3}k_x)\cos(k_y)$$

are the basis functions of the s-wave symmetry. Since singlet superconductivity with the d-wave order parameter symmetry is realized in $Na_xCoO_2 \cdot yH_2O$, we will henceforth (for brevity) confine our analysis to only the representation of the contributions to the anomalous component of the mass operator, which ensure the above symmetry. Then the graphic representation of $\Delta(k)$ is given by the sum of sever diagrams shown in Fig. 1.

The solid curves in the diagrams with a light (dark) arrow denote anomalous Green functions $G_{\downarrow 2,2\uparrow}(q, i\omega_l) = F(q, i\omega_l)$ and $G_{\uparrow 2,2\downarrow}(q, i\omega_l) = -F(-q, -i\omega_l)$, respectively.

The fine line with a light (dark) arrow denotes the initial propagator for the upper Hubbard subband of a Fermi particle with the "up" ("down") spin.

The light (dark) circle corresponds to end factor $N_{2\uparrow}$ ($N_{2\downarrow}$), where $N_{2\sigma} = N_2 + N_\sigma$, $N_\sigma = \langle X_f^{\sigma\sigma} \rangle$ is the occupation number of the single-site state with one electron with spin projection σ, and $N_2 = \langle X_f^{22} \rangle$ is the occupation number of the single-site state with two electrons. Their values for the spin-singlet superconducting phase coincide, $N_{2\uparrow} = N_{2\downarrow} = (1 + x)/2$.

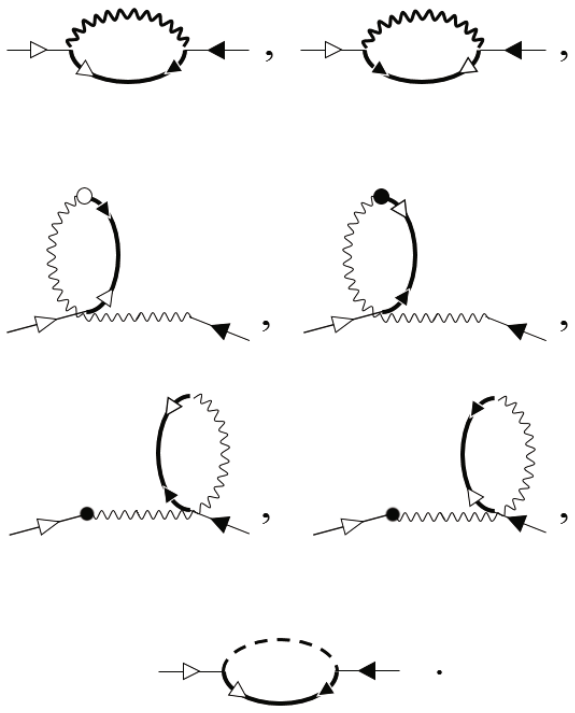

Fig. 1. Diagrams for order parameter $\Delta(k)$.

Two diagrams in the upper row determine the contributions to $\Delta(k)$, which are associated with the exchange interaction described by operator $\hat{J}$. The bold wavy curves in the diagram correspond to Fourier transform J_q of the parameters of intersite exchange interaction J_{fg}.

The next four diagrams in the second and third rows describe correlated hops reflected in H_{eff} by three-center terms in expression (6). As shown in [35], the total contribution of the first six diagrams to the equation for the order parameter with the d-wave symmetry can be written in the form of the contribution from only two first diagrams if we take for the effective coupling constant the renormalized exchange $\tilde{J}_q$:

$$J_q \to \tilde{J}_q = J_q - J_q N_{2\sigma} = \frac{1-x}{2} J_q. \quad (16)$$

The seventh diagram corresponds to the contribution to $\Delta(k)$ from the intersite Coulomb interaction of fermions. Fourier transform V_q of this interaction is shown by the bold dashed curve.

Comparing the diagrams with analytic expressions and taking into account the above renormalizations as well as the above expressions for the anomalous Green functions, we obtain the following self-consistency equation for the $(d + id)$-wave order parameter symmetry:

$$\Delta(k) = \frac{1}{N}\sum_q \left(\frac{1-x}{2}(J_{k+q} + J_{k-q}) - V_{k-q}\right) \times \Delta(q)\frac{\tanh(E_q/2T)}{2E_q}. \quad (17)$$

In deriving this equation, we have preliminarily performed summation over the Matsubara frequencies using the structure of function $F(q, i\omega_l)$.

4. TEMPERATURE OF TRANSITION TO THE CHIRAL SUPERCONDUCTING ($d + id$)-WAVE PHASE IN THE 2D HUBBARD FERMION ENSEMBLE

We can easily find the solution to Eq. (17) assuming that the kernel of this integral equation can be written in the split form. In the 2D case with a triangular lattice, when the dynamics of Hubbard fermions is determined by their hops and the intersite interaction, the splitting follows from the Fourier representation of intersite interactions.

Considering the exchange and Coulomb interactions within two coordination spheres the parameterization of which is determined by quantities J_1, J_2 and V_1, V_2, respectively, this representation can be written in form

$$J_q = 2J_1\varphi_{s1}(q) + 2J_2\varphi_{s2}(q),$$
$$V_q = 2V_1\varphi_{s1}(q) + 2V_2\varphi_{s2}(q),$$

where $\varphi_{si}(q)$ are the basis functions defined by expressions (15). The form of the analytic dependence $\Delta_d(k)$ on the quasi-momentum is determined by the basis functions of the pairing potentials, which are transformed in accordance to the irreducible d-wave representation of rotation group C_6.

Such basis functions for a triangular lattice are chiral by nature and complex-valued. If the range of the pairing potentials is bounded by two coordination spheres, it is sufficient to use the following two functions as the basis [11]:

$$\varphi_{d1}(k) = \cos k_y - \cos\left(\frac{\sqrt{3}k_x}{2}\right)\cos\left(\frac{k_y}{2}\right) + i\sqrt{3}\sin\left(\frac{\sqrt{3}k_x}{2}\right)\sin\left(\frac{k_y}{2}\right), \quad (18)$$

$$\varphi_{d2}(k) = \cos\sqrt{3}k_x - \cos\left(\frac{\sqrt{3}k_x}{2}\right)\cos\left(\frac{3k_y}{2}\right) - i\sqrt{3}\sin\left(\frac{\sqrt{3}k_x}{2}\right)\sin\left(\frac{3k_y}{2}\right). \quad (19)$$

Then the chiral ($d + id$)-wave order parameter can be written in the form of superposition

$$\Delta_d(k) = 2\Delta^0_{d1}\varphi_{d1}(k) + 2\Delta^0_{d2}\varphi_{d2}(k). \quad (20)$$

Ultimately, the problem is reduced to solving the system of two transcendental equations in unknown amplitudes Δ^0_{d1} and Δ^0_{d2}:

$$(1 - A_{11})\Delta^0_{d1} - A_{12}\Delta^0_{d2} = 0,$$
$$-A_{21}\Delta^0_{d1} + (1 - A_{22})\Delta^0_{d2} = 0, \quad (21)$$

which is obtained by substituting solution $\Delta_d(k)$ in form (20) into Eq. (17). Coefficients A_{ij} of this system are defined as

$$A_{11} = (\alpha J_1 - V_1)\frac{1}{N}\sum_q \cos\left(\frac{\sqrt{3}}{2}q_x + \frac{1}{2}q_y\right) \times\left[\cos\left(\frac{\sqrt{3}}{2}q_x + \frac{1}{2}q_y\right) - \cos q_y\right]L_q,$$

$$A_{12} = (\alpha J_1 - V_1)\frac{1}{N}\sum_q \cos\left(\frac{\sqrt{3}}{2}q_x + \frac{1}{2}q_y\right) \times\left[\cos\left(\frac{\sqrt{3}}{2}q_x - \frac{3}{2}q_y\right) - \cos\sqrt{3}q_x\right]L_q, \quad (22)$$

$$A_{22} = (\alpha J_2 - V_2)\frac{1}{N}\sum_q \cos(\sqrt{3}q_x) \times\left[\cos(\sqrt{3}q_x) - \cos\left(\frac{\sqrt{3}}{2}q_x + \frac{3}{2}q_y\right)\right]L_q,$$

$$A_{21} = (\alpha J_2 - V_2)\frac{1}{N}\sum_q \cos(\sqrt{3}q_x) \times\left[\cos q_y - \cos\left(\frac{\sqrt{3}}{2}q_x + \frac{1}{2}q_y\right)\right]L_q,$$

where $L_q = \tanh(E_q/2T)/E_q$.

To demonstrate the role of correlated hops in the formation of properties of the superconducting phase, we have introduced renormalization factor α in exchange interaction parameters. In the case when correlated hops are disregarded (t–J–V model), $\alpha = 2$ and ξ_q is defined by expressions (12). If, however, these hops are considered (t–J^*–V model), coefficient $\alpha = 1 - x$, and the spectrum is determined from relation (13).

Since quantities V_i and J_i appear additively in the Eqs. (22) for the order parameter, we will henceforth assume that $V_2 = 0$.

Relations (21) lead to the following equation for determining the superconducting transition temperature:

$$(1 - A^0_{11}) - (1 - A^0_{22}) - A^0_{12}A^0_{21} = 0, \quad (23)$$

in which quantities A^0_{ij} differ from A_{ij} only in that spectrum E_q appearing in quantity L_q is taken for $\Delta_q \equiv 0$.

Figure 2 demonstrates the effect of Coulomb correlations on the concentration dependence of the superconducting transition temperature for the phase

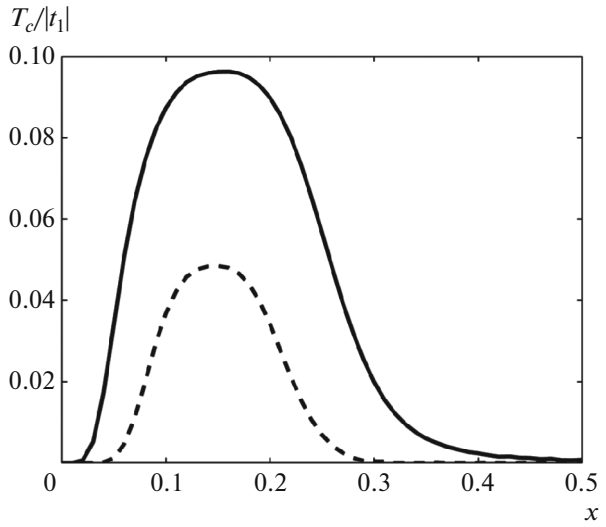

Fig. 2. Dependences of the superconducting transition temperature in the chiral superconducting phase on the concentrations of "twos" ($x = n - 1$), obtained in the t–J–V model; solid curve corresponds to $V_1 = 0$, dashed curve, to $V_1 = 0.3$; $J_1 = 0.3$, $J_2 = 0.2$, $t_2 = t_3 = 0$ (here and below, all parameters are given in the units of $|t_1|$).

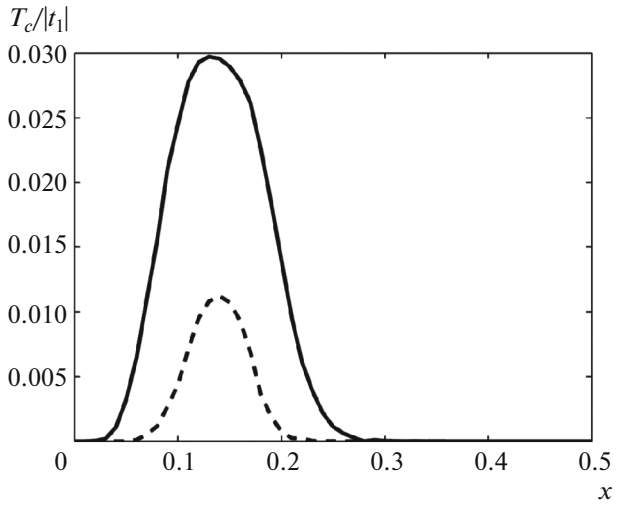

Fig. 3. Dependences of the superconducting transition temperature in the chiral superconducting phase on the concentrations of "twos" obtained in the t–J^*–V model; solid curve corresponds to $V_1 = 0$, dashed curve, to $V_1 = 0.15$; $J_1 = 0.3$, $J_2 = 0.2$, $t_2 = t_3 = 0$.

with the chiral ($d + id$)-wave symmetry for the t–J–V model. The renormalization associated with the inclusion of transcendental terms reduces the superconducting transition temperature and the region of realization of the superconducting phase (Fig. 3). The solid curve in both figures corresponds to the case when the Coulomb correlations are disregarded ($V_1 = V_2 = 0$). As expected, the Coulomb repulsion of fermions suppresses the Cooper instability. At the same time, it is significant that representation of $\Delta_d(k)$ in terms of the two basis functions may lead to the following important effect: in the case of pairing suppression in one coordination sphere, the superconducting phase can remain stable owing to pairing in the other coordination sphere. In this case, the relative contributions from two chiral invariants to $\Delta_d(k)$ are noticeably redistributed. This determines the mechanism governing the effect of the intersite Coulomb interaction on the topological transition in the chiral superconducting phase of the 2D Hubbard fermion ensemble on a triangular lattice. Let us consider this effect in greater detail.

5. EFFECT OF COULOMB CORRELATIONS ON THE CONFIGURATION OF NODAL POINTS AND ITS CONCENTRATION EVOLUTION

The important role of Coulomb correlations in the problem of a quantum topological transition is associated with extension of the possibility of its realization. It is known that the topological properties of the 2D superconducting phase with complex order parameter

$$\Delta_d(k) = \mathrm{Re}\,\Delta_d(k) + i\,\mathrm{Im}\,\Delta_d(k)$$

change when the Fermi surface passes through nodal points of $\Delta_d(k)$. As shown in [11], in the presence of only one basis function corresponding to the second coordination sphere, zeros of $\Delta_d(k)$ lie within the Brillouin zone at geometrically fixed points. Consequently, a quantum topological transition occurs only for the fermion concentration that is an independent quantity. In this case, it is difficult to realize the gapless phase for the concentration corresponding to the experimental value.

A different situation is observed when the Coulomb correlations and exchange interactions within two coordination spheres are taken into account. In this case, because of the superposition of two basis functions, the positions of zeros depend on the ratio of amplitudes Δ_{d1}^0 and Δ_{d2}^0 of complex parameter $\Delta_d(k)$. In this case, "old" zero may disappear, while new zeros may appear. Figure 4 demonstrates the variation of the configuration of nodal points upon a change in amplitudes Δ_{d1}^0 and Δ_{d2}^0. Since the specific values of these amplitudes change upon the variation of model parameters, the fermion concentration, and, generally, the temperature, the gapless phase and the point of the topological transition can easily be matched with the experimental point.

The concentration evolution of nodal points is of special importance. Since this evolution can change qualitatively upon the actuation of correlated hops, we consider results separately.

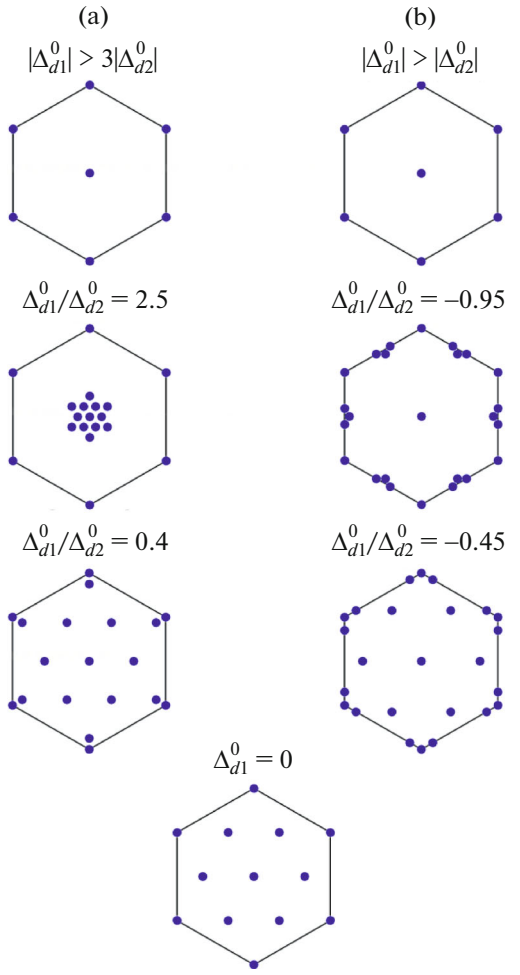

Fig. 4. (Color online) Configuration of nodal points of order parameter $\Delta_d(k)$ with the chiral symmetry type for different ratios of amplitudes Δ^0_{d1} and Δ^0_{d2}: (a) amplitudes have the same sign; (b) amplitude have opposite signs.

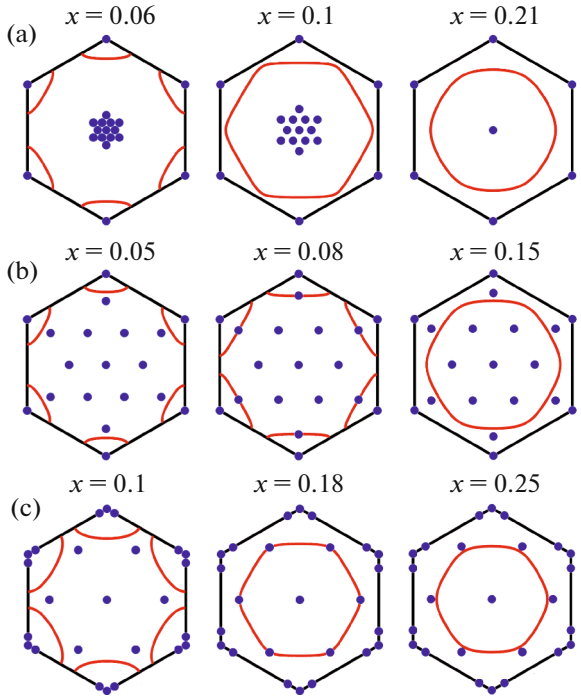

Fig. 5. (Color online) Configuration of nodal points of $\Delta_d(q)$ and of the Fermi contour for different concentrations x of "twos" in the t–J–V model: (a) $t_2 = t_3 = 0$, $V_1 = 0$; (b) $t_2 = t_3 = 0$, $V_1 = 0.3$; (c) $t_2 = 0.2$, $t_3 = 0.15$, $V_1 = 10$. In all figures, $J_1 = 0.3$ and $J_2 = 0.2$

5.1. t–J–V Model

Figure 5 shows the arrangement of the nodal points of $\Delta_d(k)$ in the Brillouin zone and the Fermi contour, which was obtained from the solution of system (21), in the t–J–V model for different parameters of the system. Figure 5a corresponds to the case when the intersite Coulomb interaction is disregarded. Upon an increase in the concentration, ratio $\Delta^0_{d1}/\Delta^0_{d2}$ changes. This causes first an insignificant "expansion" and then a displacement of nodal points towards the center of the Brillouin zone, which is stronger than the displacement of the Fermi contour. As a result, a change in the fermion concentration in this regime is not accompanied by a quantum topological transition. This is one of significant features associated with the superposition nature of the chiral order parameter.

The situation may change significantly when the Coulomb correlations are taken into account. In spite of the fact that the position of the Fermi contour is independent of the Coulomb interaction, the mutual dynamics of the nodal points and the Fermi contour changes qualitatively (Fig. 5b) in the case when V_1 (Coulomb electron interaction parameter) is close to the value of J_1 (exchange coupling parameter for the nearest sites), and the Coulomb electron interaction parameter V_2 for the second coordination sphere equals zero. In this case, nodal points are shifted relatively slowly, and the Fermi contour has time to catch up with it. At the critical concentration, the system of nodal points of $\Delta_d(k)$ lies on the Fermi contour.

Thus, the inclusion of the Coulomb correlations between the Hubbard fermions from the first coordination sphere not simply suppresses the tendency to pairing, but may substantially affect the dynamics of nodal points by modifying partial amplitudes Δ^0_{d1} and Δ^0_{d2} and, hence, initiate a topological quantum transition to the superconducting state.

For $V_1 \gg J_1$, the system of nodal points becomes close to the system determined exclusively by the second basis function, and the concentration behavior of the system corresponds to the scenario described in [11], the enhancement of the Coulomb interaction is manifested only in the decrease in the transition temperature in the range of realization of the superconducting phase, but does not change the position of the

nodal points. In Fig. 5c, the parameters of the system are such that for large values of V, the superconducting phase exists at the critical concentration.

5.2. t–J^*–V Model

The account for correlated hops causes a renormalization of the pairing interaction constant. For this reason, the superconducting transition temperature and the region of existence of the superconducting phase decrease. Another effect of the aforementioned hops is manifested in the possibility of changing the concentration dynamics of nodal points and, as a consequence, of changing the scenario of the topological transition. This is demonstrated in Fig. 6, which shows the configurations of the nodal points of $\Delta_d(k)$ in the Brillouin zone in different conditions. In the absence of Coulomb correlations (Fig. 6a), the behavior of the nodal points in the t–J^*–V model does not differ qualitatively from the behavior of these points in the t–J model. Therefore, the Fermi contour does not intersect nodal points either, and no quantum topological transition occurs. When the intersite interaction due to the renormalization of the exchange interaction is considered, the first scenario of the formation of the phase with a gapless spectrum (Fig. 6b) is observed for $V_1 \sim J_1/2$, and the reduction of the region of existence of the superconducting phase rules out the second scenario of formation of the gapless phase (for $V_1 \gg J_1$) in the t–J^*–V model.

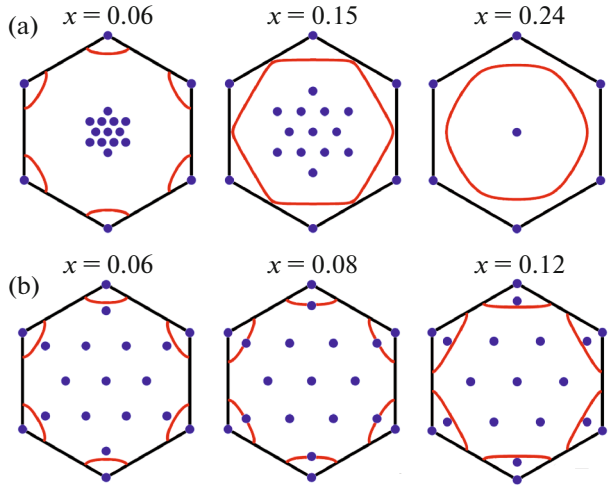

Fig. 6. (Color online) Configuration of nodal points of $\Delta_d(q)$ and of the Fermi contour for different concentrations x of "twos" in the t–J^*–V model: (a) intersite correlations are absent ($V_1 = 0$); (b) intersite correlations are activated ($V_1 = 0.15$); $J_1 = 0.3$, $J_2 = 0.2$, $t_2 = t_3 = 0$.

6. EFFECT OF INTERPLANAR HOPS ON THE FORMATION OF THE GAPLESS CHIRAL SUPERCONDUCTING ($d + id$)-WAVE PHASE

In analysis of the effect of quasi-two-dimensionality on the spectral characteristics of the superconducting phase, we consider the factors existing, for example, for sodium cobaltite. The main peculiarity is due to the fact that intercalation with water (a superconducting transition occurs precisely in this case) causes the separation of CoO_2 layers (water molecules are implanted between these layers). Consequently, the fermion hopping integral between the sites belonging to different layers becomes much smaller than the corresponding hopping integral in the plane of the layers: $|t_\perp| \ll |t|$, where $t_\perp$ is the parameter of electron hopping between the nearest sites in the direction perpendicular to the layer and $|t|$ is the largest electron hopping integral in the plane of the layer.

As a result, the interaction between magnetically active ions belonging to one layer, which is proportional to the square of the hopping parameter, is much stronger than the analogous interaction between ions from different layers. This allows us to use the approximation in which the Fermi excitation spectrum of the normal phase is calculated for the quasi-2D case, while the 3D system relative to the superconducting pairing potential is treated as a set of uncoupled layers with triangular lattices.

The intercalated water molecules are known to be implanted between CoO_2 layers. This increases the spacing between these layers. Therefore, the joint effect of the large separation between the layers and the presence of molecules with a high polarization activity in the interlayer space lead to effects of strong screening of the Coulomb potential in the direction perpendicular to the layers. It follows hence that the Coulomb interaction of fermions located in different layers can be disregarded in the main approximation.

For simplicity, we will ignore below the effect of correlated hops. Then equation (17) for calculating the superconducting order parameter formally remains unchanged; however, the expression for the Fourier transform of hopping integral (14) is supplemented with term $2t_z\cos(k_z)$.

Figure 7a demonstrates the effect of interplanar hops on the concentration dependence of the superconducting transition temperature to the chiral phase with the ($d + id$)-wave order parameter symmetry; Fig. 7b shows the effect of these hops on the density of states for the energy value equal to the chemical potential.

It can be seen that an increase in t_z leads to a decrease in the superconducting transition temperature. It should be noted, however, that the variation of T_c with increasing t_z is nonmonotonic and depends on the concentration (we are grateful to the reviewer who paid attention to this circumstance). In the optimal doping region, T_c decreases with increasing t_z, while the inverse process occurs in the overdoped region.

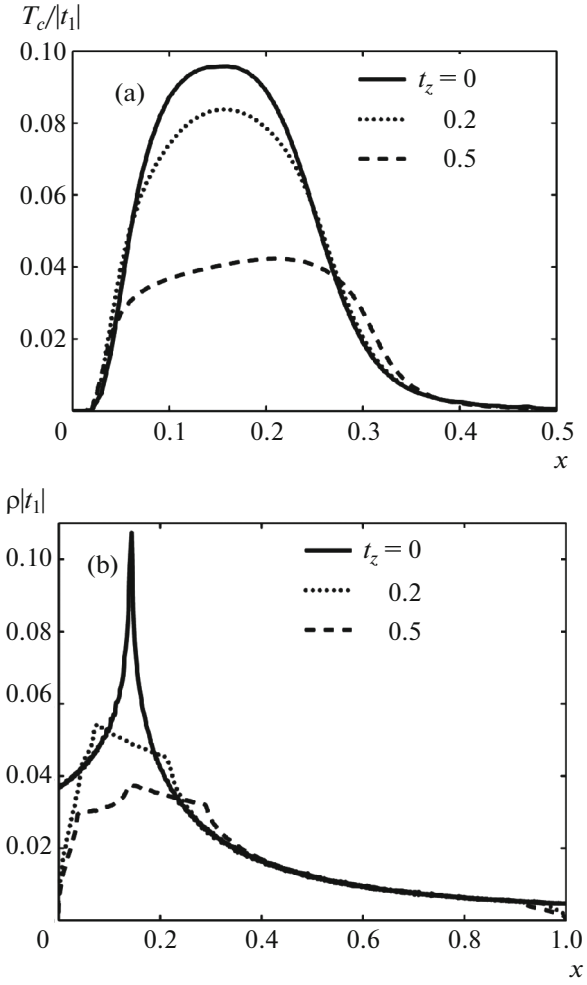

Fig. 7. (a) Dependences of the superconducting transition temperature to the chiral superconducting phase in the Hubbard fermion ensemble on the concentration of "twos" for different values of t_z; (b) Concentration dependence of the density of states at the chemical potential level for the same ensemble; $J_1 = 0.3$, $J_2 = 0.2$, $t_2 = t_3 = 0$.

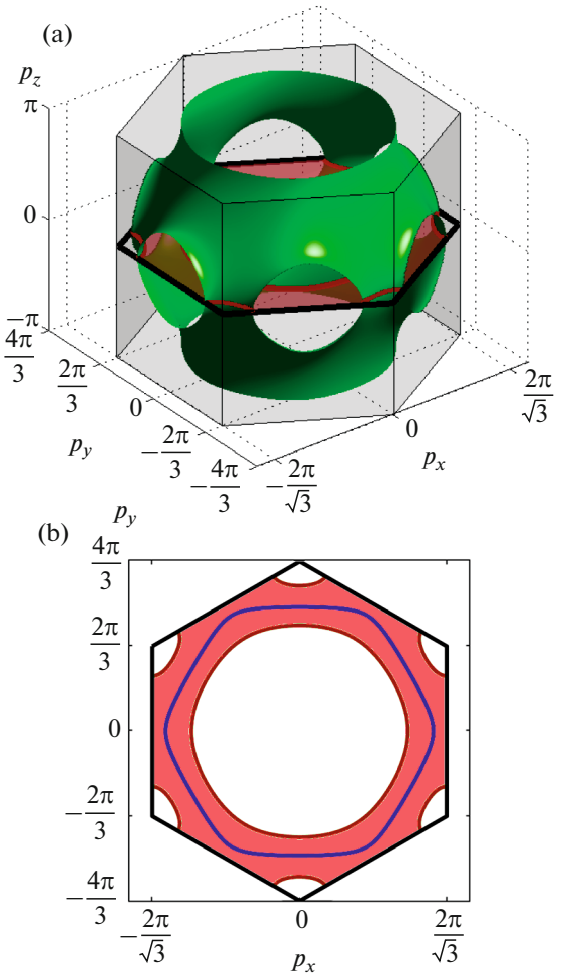

Fig. 8. (Color online) (a) Fermi surface for a quasi-2D ensemble of the Hubbard fermions ($t_z = 0.5$); (b) projection of the Fermi surface of the same ensemble onto the (p_x, p_y) plane. Concentration $x = 0.18$. The remaining parameters are the same as in Fig. 7.

Such a behavior is associated with the modification of density of states, which is manifested in blurring of the logarithmic divergence observed in the 2D system, as well as with a nonmonotonic (in concentration) variation of the density of states at the chemical potential level. A significant change in the superconducting transition temperature occurs only for values of t_z close to $0.5|t_1|$. The region of existence of the superconducting phase changes insignificantly in this case.

Since the elementary excitation spectrum acquires the dependence on p_z, and order parameter $\Delta_d(p)$ depends only on p_x and p_y upon the actuation on interplanar hops, it is more convenient in analysis of the conditions for the formation of the gapless phase to consider not the Femi surface itself, but its projection on the (p_x, p_y) plane (see Fig. 8). The blue curve in Fig. 8b shows the Fermi contour at $t_z = 0$ (2D system), and the red region appears in projecting the Fermi surface plotted for the same concentration and model parameters, but for $t_z = 0.5|t_1|$. The value of this parameter was increased for better visualization. In calculating the concentration dependence of the gap width, we will take a more realistic value. Therefore, if we include the interplanar hops, we must consider (instead of the individual Fermi contour in the pure 2D case) the surface, the width of projection of which onto the (p_x, p_y) plane is proportional to t_z.

For further analysis, it is significant that the positions of nodal points of $\Delta_d(p)$, which is determined by parameter $\Delta^0_{d2}/\Delta^0_{d1}$ (see Fig. 4), weakly depends on the interplanar hopping integral. This is demonstrated in Fig. 9. It follows hence that the main influence of the quasi-two-dimensionality effect on the system is manifested in the emergence of a finite width of the projection of the Fermi surface in the (p_x, p_y) plane. As a

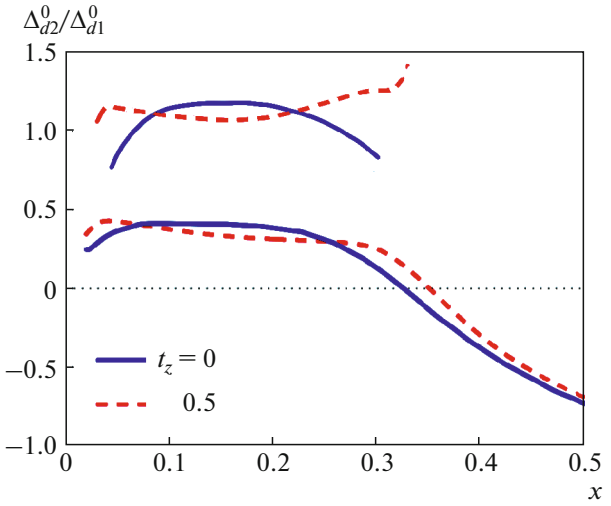

Fig. 9. (Color online) Dependences of ratio $\Delta^0_{d2}/\Delta^0_{d1}$ on the concentration in the t–J–V model for different values of t_z and V_1. Solid curves correspond to $t_z = 0$; dashed curve, to $t_z = 0.5$; lower curves were calculated for $V_1 = 0$ and upper curves, for $V_1 = 0.3$; $J_1 = 0.3$, $J_2 = 0.2$, $t_2 = t_3 = 0$.

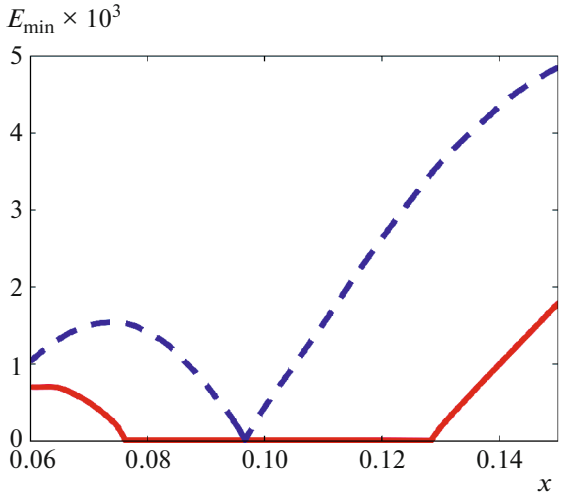

Fig. 10. (Color online) Dependences of the gap in the Fermi excitation spectrum in the superconducting phase on concentration at $t_z = 0$ (dashed curve) and $t_z = 0.1$ (solid curve); $J_1 = 0.3$, $J_2 = 0.2$, $V_1 = 0.3$; $t_2 = t_3 = 0$.

result, the superconducting phase with a gapless spectrum will be observed not at one concentration (critical point), but in a wide range of concentrations (Fig. 10). Analogously, the expansion of the surface leads to an increase in the range of values of the intersite Coulomb interaction, at which the gapless spectrum is realized. For example, for $t_2 = t_3 = 0$, $J_1 = 0.3$, $J_2 = 0.2$, and $t_z = 0.2$, the first scenario of the formation of the gapless phase (see Fig. 5b) is realized for $V_1 \in (0.2, 0.5)$.

The inclusion of hops between layers also favors the second scenario of the formation of the gapless phase, which is realized for large values of the intersite Coulomb repulsion (see Fig. 5c). The positions of the nodal points in this scenario almost coincide with zeros of basis function $\varphi_{d2}(p)$, and the Fermi surface intersects them at lower concentrations because of "broadening." For $t_2 = t_3 = 0$ and for t_z increasing from 0 to 0.5, the minimal concentration at which this intersection occurs decreases from 0.43 to 0.29.

7. CONCLUSIONS

We have analyzed the conditions in which the spectrum of the superconducting phase with the chiral order parameter becomes gapless for the quasi-2D ensemble of the Hubbard fermions on a triangular lattice with account for the interaction within two coordination spheres. It is shown that there are two scenarios for the formation of the gapless phase.

The first of them is realized in the case when the intersite Coulomb interaction parameters are comparable with the exchange interaction parameters. Then basis functions $\varphi_{d1}(p)$ and $\varphi_{d2}(p)$ give approximately identical contributions to chiral order parameter $\Delta_d(p)$. In this case, the positions of the nodal points strongly depend both on the parameters of the system and on the concentration, and the realization of the gapless phase is determined by the relative dynamics of the nodal points and the Fermi contour.

The second scenario is realized for $V_1 \gg J_1$. The positions of the nodal points are almost fully determined by only one basis function $\varphi_{d2}(p)$. The order parameter zeros lie within the Brillouin zone, and their positions weakly depend on the concentration. If superconductivity exists for the concentration at which the Fermi contour of the normal phase crosses these points, the phase with a gapless spectrum is realized. However, this situation takes place only for one value of fermion concentration, and precisely this situation was considered in [11].

The inclusion of correlated hops leads to a decrease in the region of realization of the superconducting phase; as a result, superconductivity degrades sooner than the Fermi contour intersects zeros of basis function $\varphi_{d2}(p)$ and, hence, the second scenario is not realized in the t–J^*–V model.

It is shown that a transition to the quasi-2D ensemble of the Hubbard fermions, when interplanar transitions are taken into account, the gapless superconducting chiral $(d + id)$-wave phase is realized not at a single value of concentration, but in its certain range. The expansion of the concentration range leads to the reduction of requirements of realization of the gapless phase, and both scenarios considered above are realized in a large range of parameters.

FUNDING

This study was supported by the Russian Foundation for Basic Research (project nos. 19-02-00348 and 18-42-240014), the Administration of the Krasnoyarsk Kray, the Krasnoyarsk Kray Science Foundation within research project "Single-orbital Effective Model of Ensemble of Spin-Polaron Quasiparticles in the Problem of Description of the Intermediate State and Pseudogap Behavior of Cuprate Superconductors" (project no. 18-42-240014).

REFERENCES

1. R. S. Gekht, Sov. Phys. Usp. **32**, 871 (1989).
2. D. I. Golosov and A. V. Chubukov, JETP Lett. **50**, 451 (1989).
3. A. V. Chubukov and D. I. Golosov, J. Phys.: Condens. Matter **3**, 69 (1991).
4. L. E. Svistov, A. I. Smirnov, L. A. Prozorova, O. A. Petrenko, A. Micheler, N. Buttgen, A. Ya. Shapiro, and L. N. Demianets, Phys. Rev. **74**, 024412 (2006).
5. A. I. Smirnov, T. A. Soldatov, O. A. Petrenko, A. Takata, T. Kida, M. Hagiwara, A. Ya. Shapiro, and M. E. Zhitomirsky, Phys. Rev. Lett. **119**, 047204 (2017).
6. T. A. Soldatov, A. I. Smirnov, K. Y. Povarov, M. Halg, W. E. A. Lorenz, and A. Zheludev, Phys. Rev. B **98**, 144440 (2018).
7. D. M. Dzebisashvili and A. A. Khudaiberdyev, JETP Lett. **108**, 189 (2018).
8. O. A. Starykh, Rep. Progr. Phys. **78**, 052592 (2015).
9. A. I. Smirnov, Phys. Usp. **59**, 564 (2016).
10. K. Takada, H. Sakurai, E. Takayama-Muromachi, F. Izumi, R. A. Dilanian, and T. Sasaki, Nature (London, U.K.) **422**, 53 (2003).
11. S. Zhou and Z. Wang, Phys. Rev. Lett. **100**, 217002 (2008).
12. Y.-M. Lu and Z. Wang, Phys. Rev. Lett. **110**, 096403 (2013).
13. V. V. Val'kov, A. O. Zlotnikov, and M. S. Shustin, J. Magn. Magn. Mater. **459**, 112 (2018).
14. V. V. Val'kov and A. O. Zlotnikov, JETP Lett. **109**, 736 (2019).
15. V. V. Val'kov, V. A. Mitskan, A. O. Zlotnikov, M. S. Shustin, and S. V. Aksenov, JETP Lett. **110**, 140 (2019).
16. S. Feng, Y. Lan, H. Zhao, L. Kuang, L. Qin, and X. Ma, Int. J. Mod. Phys. B **29**, 1530009 (2015).
17. X. Ma, L. Qin, H. Zhao, Y. Lan, and S. Feng, J. Low Temp. Phys. **183**, 329 (2016).
18. L. Qin, X. Ma, L. Kuang, J. Qon, and S. Feng, J. Low Temp. Phys. **181**, 112 (2015).
19. J. Hubbard, Proc. R. Soc. London, Ser. A **276**, 238 (1963).
20. M. Ye and A. Chubukov, Phys. Rev. B **100**, 035135 (2019).
21. K. S. Chen, Z. Y. Meng, U. Yu, S. Yang, M. Jarrell, and J. Moreno, Phys. Rev. B **88**, 041103(R) (2013).
22. G.-Q. Zheng et al., J. Phys.: Condens. Matter **18**, L63 (2006).
23. A. Kanigel et al., Phys. Rev. Lett. **92**, 257007 (2004).
24. H. D. Yang et al., Phys. Rev. B **71**, 020504R (2005).
25. G.-Q. Zheng et al., Phys. Rev. B **73**, 180503R (2006).
26. G. Baskaran, Phys. Rev. Lett. **91**, 097003 (2003).
27. B. Kumar and B. S. Shastry, Phys. Rev. B **68**, 104508 (2005).
28. M. Ogata, J. Phys. Soc. Jpn. **72**, 1839 (2003).
29. K. S. Chen, Z. Y. Meng, U. Yu, S. Yang, M. Jarrell, and J. Moreno, Phys. Rev. B **88**, 041103 (2013).
30. Y. Yanase, M. Mochizuki, and M. Ogata, J. Phys. Soc. Jpn. **74**, 430 (2005).
31. M. Ogata, J. Phys.: Condens. Matter **19**, 145282 (2007).
32. N. B. Ivanova, S. G. Ovchinnikov, M. M. Korshunov, I. M. Eremin, and N. V. Kazak, Phys. Usp. **52**, 789 (2009).
33. N. M. Plakida, *High-Temperature Superconductivity* (Springer, Berlin, 1995).
34. Yu. A. Izyumov, Phys. Usp. **40**, 445 (1997).
35. V. V. Val'kov, T. A. Val'kova, D. M. Dzebisashvili, and S. G. Ovchinnikov, JETP Lett. **75**, 378 (2002).
36. V. V. Val'kov, T. A. Val'kova, and V. A. Mitskan, JETP Lett. **102**, 361 (2015).
37. S. P. Shubin and S. V. Vonsovsky, Proc. R. Soc. London, Ser. A **145**, 159 (1934).
38. S. P. Shubin and S. V. Vonsovsky, Phys. Z. Sowjetunion **7**, 292 (1935).
39. S. P. Shubin and S. V. Vonsovsky, Phys. Z. Sowjetunion **10**, 348 (1936).
40. N. N. Bogolyubov, *Selected Works, in 3 Volumes* (Naukova Dumka, Kiev, 1970), Vol. 2 [in Russian].
41. R. O. Zaitsev, Sov. Phys. JETP **41**, 100 (1975); Sov. Phys. JETP **43**, 574 (1976).
42. R. O. Zaitsev, *Diagram Methods in the Theory of Superconductivity and Ferromagnetism* (URSS, Moscow, 2004) [in Russian].
43. V. V. Val'kov and A. A. Golovnya, J. Exp. Theor. Phys. **107**, 996 (2008).
44. L. P. Gor'kov, Sov. Phys. JETP **7**, 505 (1958).

Translated by N. Wadhwa